

## Electronic supporting information for

### A portable fluorescence detection device based on a smartphone employing carbon nanodots for Mn<sup>2+</sup> sensing

Pijika Mool-am-kha<sup>a</sup>, Samuch Phetduang<sup>a</sup>, Kessarinn Ngamdee<sup>a</sup>,  
Chayada Surawanitkun<sup>d</sup>, Xiang-Kui Ren<sup>d</sup>, Wittaya Ngeontae<sup>a,b,c\*</sup>

<sup>a</sup>*Department of Chemistry, Faculty of Science, Khon Kaen University, Khon Kaen 40002,  
Thailand*

<sup>b</sup>*Research Center for Environmental and Hazardous Substance Management (EHSM), Khon  
Kaen University, Khon Kaen 40002, Thailand*

<sup>c</sup>*Faculty of Interdisciplinary Studies, Khon Kaen University, Nong Khai Campus, Nong Khai  
43000, Thailand*

<sup>d</sup>*School of Chemical Engineering and Technology, State Key Laboratory of Chemical  
Engineering, Tianjin University, Tianjin 300350, P. R. China*

#### Corresponding authors:

Wittaya Ngeontae\* E-mail: [wittayange@kku.ac.th](mailto:wittayange@kku.ac.th)

## 1. Synthesis of N,S-CDs

N,S-CDs were synthesized through pyrolysis of lactose and L-cysteine by following previously reported [R1]. Briefly, 0.4000 g of lactose and 0.1000 g of L-cysteine were homogeneously dissolved by 8 mL of sodium hydroxide solution with continuous stirring. Subsequently, the mixed solution was heated at 90°C on a hotplate for 5 minutes. The color of the mixture solution was changed from colorless to light yellow and brown, then left at room temperature, and finally, deionized water into the brown solution to a total volume of 16.00 mL. Parallely, the CDs were synthesized by the same procedure as N,S-CDs but without adding L-cysteine.

## 2. Characterization of the N,S-CDs

The N,S-CDs underwent pyrolysis in a highly alkaline solution, utilizing lactose as a carbon precursor and L-cysteine as the source of N and S atoms. The undoped CDs, which serve as a comparison, were produced using the same process but without including L-cysteine. The yielded products performed complete characterization in previous studies [R1]. The morphology of N,S-CDs was investigated using a transmission electron microscope (TEM). The N,S-CDs exhibited a spherical morphology and a narrow size distribution. The average particle size, measured by the ImageJ program as shown in Fig. S1(a), was around  $3.1 \pm 0.4$  nm. The UV-visible and fluorescence spectrometer were utilized to investigate the optical characteristics of the N,S-CDs. The absorption of N,S-CDs demonstrates a distinctive absorption peak at a wavelength of 301 nm. Additionally, the peak of shoulder absorption appeared at a wavelength of 330 nm, which can be attributed to the transition of electrons in the carbon nanostructure, specifically the  $\pi-\pi^*$  or  $n-\pi^*$  transition [R2]. The absorption peak of the N,S-CDs exhibited a distinct distinctive peak in contrast with ordinary CDs, as illustrated in Fig. S1(b). In addition, the fluorescence emission characteristic of the N,S-CDs was examined, as represented in Fig. S1(c). The characteristic excitation and emission wavelengths of N,S-CDs were observed to be 420 and 513 nm, respectively. Furthermore, Fourier Transform Infrared (FT-IR) spectroscopy was employed to analyze the constituent functional groups inside the N,S-CDs, as depicted in Fig. S1(d). The peak at  $3573.9 \text{ cm}^{-1}$  corresponds to the stretching vibrations of the O-H bond, while the broad absorption band at  $2819.8 \text{ cm}^{-1}$  indicates the presence of O-H and carboxylic acid groups. Additionally, the signal observed at a wavenumber of  $1570.0 \text{ cm}^{-1}$  can be attributed to the presence of the O-C-O functional group. The  $1415.2 \text{ cm}^{-1}$  peak indicates the distinctive  $-\text{CH}_2-$  chain structure. Furthermore, the presence of N-H and C-N functional groups was verified by observing characteristic peaks at  $1741.65$  and  $1217.0 \text{ cm}^{-1}$ , respectively. The results obtained from these approaches confirm the successful preparation of N,S-CDs.

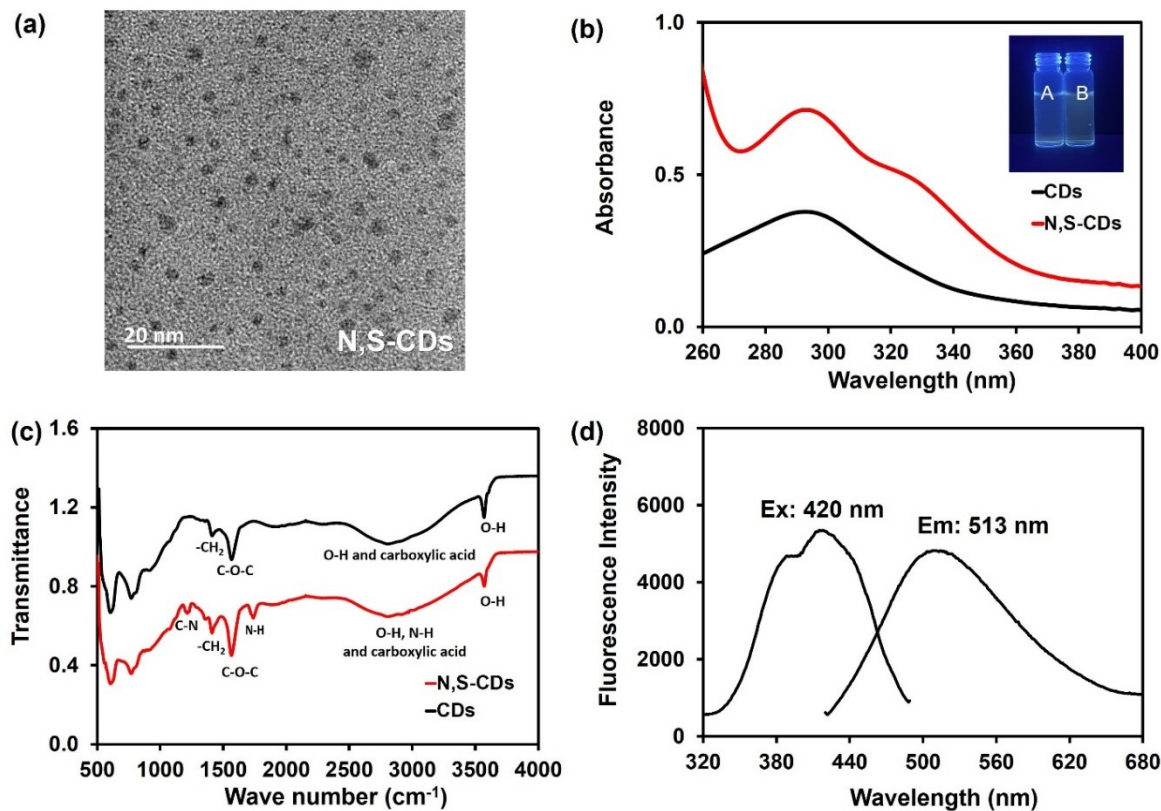


**Fig. S1** (a) TEM image of the N,S-CDs, (b) UV-Vis absorption spectra of CDs and N,S-CDs (inset: photographs of CDs (A) and N,S-CDs (B)) under UV irradiation), (c) FT-IR spectrum of CDs and N,S-CDs, (d) fluorescence excitation and emission spectrum of the N,S-CDs at excitation wavelength of 420 nm.

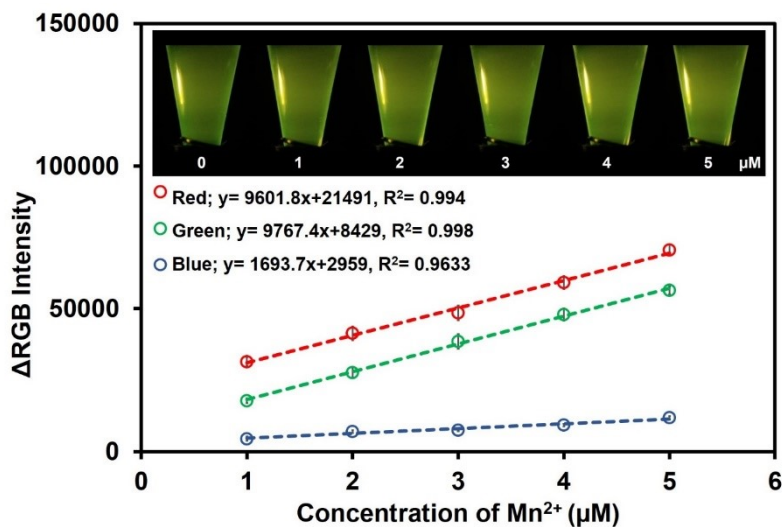


**Fig. S2** Linear calibration graph and images of solutions acquired by the smartphone camera for detecting  $Mn^{2+}$  in the 0.1 M acetic-acetate buffer (pH 5.0).

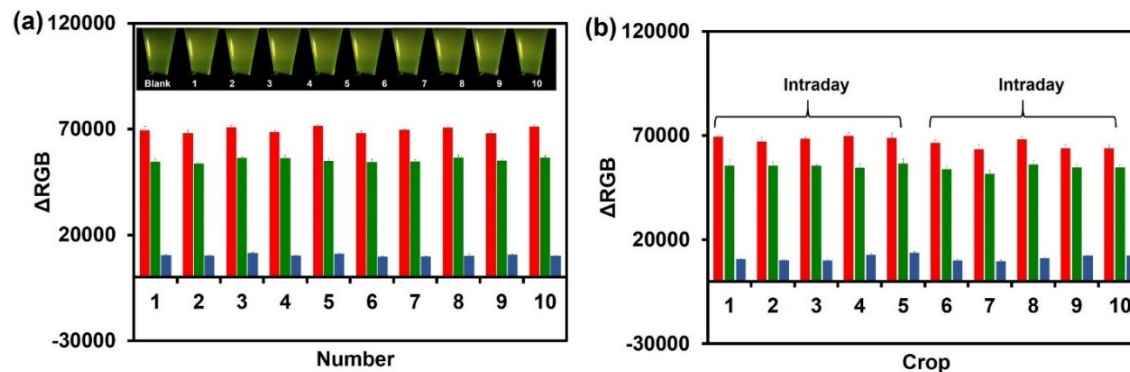


**Fig. S3** The  $\Delta$ RGB intensities determined from (a) the same crop and (b) the different crop on the same day and a different day of N,S-CDs in the presence of 5  $\mu$ M measured in the 0.1 M acetic-acetate buffer (pH 5.0) using a smartphone.

**Table S1** The performance characteristics comparison of smartphone-based portable fluorescence sensor as metal ion sensing

Materials	Target analytes	Working range ( $\mu$ M)	Detection limit ( $\mu$ M)	Samples	[Ref.]
Carbon dots	Pb <sup>2+</sup>	0-0.200	0.00289	Tap water, lake water	[R3]
Carbon dots	Hg <sup>2+</sup> , Pb <sup>2+</sup> , Cu <sup>2+</sup>	0.020-0.320(Hg <sup>2+</sup> ), 0.2-6.4 (Pb <sup>2+</sup> ), 0.125–2(Cu <sup>2+</sup> )	0.0058 (Hg <sup>2+</sup> ), 0.12 (Pb <sup>2+</sup> ), 0.076 (Cu <sup>2+</sup> )	River water	[R4]
Cadmium telluride quantum dots	Ni <sup>2+</sup>	0.34-1.70 (20-100 $\mu$ gL <sup>-1</sup> )	0.11(6.2 $\mu$ gL <sup>-1</sup> )	Tea	[R5]
Carbon dots	Cu <sup>2+</sup>		0.344	-	[R6]
Rhodamine B-Gold nanoparticles	Zn <sup>2+</sup>	1.5 – 91.7 (0.1 – 6 mgL <sup>-1</sup> )	1.5 (0.1 mgL <sup>-1</sup> )	Water	[R7]
Silver nanoclusters	Hg <sup>2+</sup>	0.050-2.50 (0.010 - 0.5 $\mu$ g mL <sup>-1</sup> )	0.0090 (1.8 $\mu$ gL <sup>-1</sup> )	Porphyra	[R8]
N, S-doped carbon dots	Mn <sup>2+</sup>	1-5	0.5	Cosmetics	This work

**Table S2** The performance characteristics comparison of the proposed sensor with other nanomaterials-based fluorescence sensors for the determination of Mn<sup>2+</sup>

Materials	Detection Method	Working range (μM)	Detection limit (μM)	Interferences	Samples	[Ref.]
Silicon nanoparticle clusters	Fluorescence, Colorimetry	1-10	1.2	Cu <sup>2+</sup>	Fingerprints	[R9]
Silicon nanoparticles	Fluorescence	2.5-250	1.1	Fe <sup>3+</sup> , Cu <sup>2+</sup>	Tap water	[R10]
Copper nanoparticles	Fluorescence	2.5-250	1.6	Fe <sup>3+</sup> , Pt <sup>2+</sup>	-	[R11]
ZnCdS/ZnS QD/carboxymethyl chitosan/g-C <sub>3</sub> N <sub>4</sub> nanosheet nanocomposite film	Fluorescence	1.961-16.67	-	Hg <sup>2+</sup>	Water samples	[R12]
N-C QD/CCSCD nanocomposites*	Fluorescence	0-21.1	0.0053	Fe <sup>3+</sup> , Mg <sup>2+</sup>	Water samples	[R13]
N, S-doped carbon dots	Fluorescence	0-5	0.12	-	Tap water, wastewater	[R14]
Histidine functionalized carbon quantum dots	Fluorescence	0.064-0.65 (3.50–35.5 μg L <sup>-1</sup> )	0.034 (1.85 μg L <sup>-1</sup> )	-	Whole blood	[R15]
N, S-doped carbon dots	Fluorescence-based smartphone	1-5	0.5	-	Cosmetics	This work

\*N-C QD/CCSCD nanocomposites ; Carboxymethyl chitosan crosslinked with cyclodextrin containing hydrogen-bonded N-C QDs

## References

- [R1] W. Ngeontae, K. Chaiendoo, K. Ngamdee, S. Ruangchai, C. Saiyasombat, W. Busayaporn, S. Ittisanronnachai, V. Promarak, A highly selective fluorescent sensor for manganese(II) ion detection based on N,S-doped carbon dots triggered by manganese oxide, *Dyes Pigm.*, 2022, **203**, 110325.
- [R2] H. Zhu, X. Wang, Y. Li, Z. Wang, F. Yang, X. Yang, Microwave synthesis of fluorescent carbon nanoparticles with electrochemiluminescence properties, *Chem Commun.*, 2009, **34**, 5118–5120.
- [R3] H. Wang, L. Yang, S. Chu, B. Liu, Q. Zhang, L. Zou, S. Yu, C. Jiang, Semiquantitative visual detection of lead ions with a smartphone via a colorimetric paper-based analytical device, *Anal. Chem.*, 2019, **91**, 9292–9299.

- [R4] M. Xiao, Z. Liu, N. Xu, L. Jiang, M. Yang, C. Yi, A smartphone-based sensing system for on-site quantitation of multiple heavy metal ions using fluorescent carbon nanodots-based microarrays, *ACS Sens.*, 2020, **5**, 870–878.
- [R5] X. Yuan, J. Zhang, H. Yang, Q. Yang, L. Li, M. Zhang, K. Huang, Quantum dots immobilized paper for specific and sensitive quantitation of Ni(II) by headspace photochemical vapor generation: Mechanism and application for RGB detection in tea fusion with a smartphone, *Sens. Actuators B Chem.*, 2022, **372**, 132686.
- [R6] Z. Lu, M. Chen, M. Li, T. Liu, M. Sun, C. Wu, G. Su, J. Yin, M. Wu, P. Zou, L. Lin, X. Wang, Q. Huang, H. Yin, H. Rao, X. Zhou, J. Ye, Y. Wang, Smartphone-integrated multi-color ratiometric fluorescence portable optical device based on deep learning for visual monitoring of Cu<sup>2+</sup> and thiram, *Chem. Eng. J.*, 2022, **439**, 135686.
- [R7] D. Hatiboruah, S. Biswas, D. Sarma, P. Nath, A smartphone-based photometric and fluorescence sensing for accurate estimation of zinc ion in water, *Sensors Actuators A Phys.*, 2022, **341**, 113586.
- [R8] W. Li, X. Zhang, X. Hu, Y. Shi, W. Xin, N. Liang, T. Shen, J. Xiao, M. Daglia, X. Zou, J. Shi, Dual modes of fluorescence sensing and smartphone readout for sensitive and visual detection of mercury ions in Porphyra, *Anal. Chim. Acta*, 2022, **1226**, 15, 340153.
- [R9] B. Zhu, M. Tang, L. Yu, Y. Qu, F. Chai, L. Chen, H. Wu, Silicon nanoparticles: fluorescent, colorimetric and gel membrane multiple detection of Cu<sup>2+</sup> and Mn<sup>2+</sup> as well rapid visualization of latent fingerprints, *Anal. Methods*, 2019, **11**, 3570–3577.
- [R10] L. Meng, Y. Yuan, G. Pu, N. Xu, An “on–off–on” fluorescence assay based on silicon nanoparticles for selective detection of manganese(II), *Anal. Methods*, 2017, **9**, 2553–2560.
- [R11] S. Y. Ma, Y. C. Yeh, One-step synthesis of water-soluble fluorescent copper nanoparticles for label-free detection of manganese ions, *Anal. Methods*, 2015, **7**, 6475–6478.
- [R12] S. Wang, J. Liu, Y. Huang, N. Yang, Selective sensing of Mn<sup>2+</sup> based on ZnCdS/ZnS QD/carboxymethyl chitosan/g-C<sub>3</sub>N<sub>4</sub> nanosheet nanocomposite film by the conformational regulation of polymer chain, *Appl. Surf. Sci.*, 2020, **530**, 14725.
- [R13] S. Wang, J. Liu, H. Zhao, F. Zhang, Carboxymethyl chitosan crosslinked  $\beta$ -cyclodextrin containing hydrogen bonded NC QDs nanocomposites to design fluorescence probes for manganese ion (II) sensing, *Mater. Sci. Eng. C.*, 2021, **119**, 111556.
- [R14] W. Ngeontae, K. Chaiendoo, K. Ngamdee, S. Ruangchai, C. Saiyasombat, W. Busayaporn, S. Ittisanronnachai, V. Promarak, A highly selective fluorescent sensor for manganese(II) ion detection based on N,S-doped carbon dots triggered by manganese oxide, *Dyes Pigm.*, 2022, **203**, 110325.
- [R15] E. Mohagheghpour, L. Farzin, A. Ghoorchian, S. Sadjadi, M. Abdouss, Selective detection of manganese(II) ions based on the fluorescence turn-on response via histidine functionalized carbon quantum dots, *Spectrochim. Acta A*, 2022, **279** 121409.